

MOMENT RESISTANCE PERFORMANCE OF LARCH LAMINATED TIMBER BEAM-COLUMN JOINTS REINFORCED WITH CFRP¹

Dong-Hyeon Kim

Master's Student
E-mail: wrudoing0202@naver.com

Seung-Yeoup Baek

Master's Student
E-mail: bso1936@naver.com

Seok-Hoon Yu

Master's Student
Department of Forest Biomaterials Engineering
Chuncheon, Republic of Korea
E-mail: bibunm1ss@hanmail.net

Yo-Jin Song

Researcher
Institute of Forest Science
Kangwon National University
1 Gangwondaehakgil
Chuncheon-Si 24341, Republic of Korea
E-mail: syj85@kangwon.ac.kr

In-Hwan Lee

Research Fellow
Wood Engineering Division Forest Products and Industry Department
National Institute of Forest Science
57 Hoegi-ro, Dongdaemun-gu, Seoul 02455, Republic of Korea
E-mail: ih1990@korea.kr

*Soon-Il Hong**

Professor
Department of Forest Biomaterials Engineering
Kangwon National University
1 Gangwondaehakgil
Chuncheon-Si 24341, Republic of Korea
E-mail: hongsi@kangwon.ac.kr

(Received August 2021)

Abstract. Laminated timber is a wood composite made by multiple-layering of small-square timber. Laminated timber was produced as a substitute for glulam or large-section timbers. Existing studies have shown that laminated timber has potential as a structural member, but experiments on joints for using laminated timber as a structure are insufficient. Slotted-in steel plates type joint are commonly used among various types of joints for timber owing to their outstanding strength and stiffness. However, they are vulnerable to cyclic loads such as earthquakes, and to brittle fractures due to the bearing deformation of the wood given the large difference in stiffness between the wood and the joint composed of metal fasteners and steel plate. Since brittle

* Corresponding author

¹ The copyright of this article is retained by the authors.

fractures cause a large decrease in joint capacity, many studies are being conducted to solve this problem. Among them, carbon fiber-reinforced plastic (CFRP) is used as reinforcing material due to its excellent strength characteristics, but experiments on the performance of column-beam joints reinforced with CFRP joints are insufficient. Therefore, this study evaluates the moment capacity according to CFRP reinforcement ratio of the drift pin larch beam-column joint with slotted-in steel plates of larch laminated timber. The main strength characteristics and seismic performance of the joints were calculated using the elasto-plastic model. There was almost no difference in strength between the control specimens and the joints composed of glulams. The strength gain of the joints of the larch laminated timber was greater when glulam and laminated timber were reinforced with CFRP of the same volume ratio compared with CFRP reinforcement. Unlike the specimens wrapped in CFRP in the previous study, the moment of resistance specimens reinforced with CFRP were improved without any reduction in yield strength and ductility ratio, and it was confirmed that the failure mode was improved. Through the experimental results, it was confirmed that the internal reinforcement method of CFRP contributes to the performance improvement of the joint.

Keywords: Laminated timber, timber dowel-type joints, reinforcement, elasto-plastic analysis, failure mode, ductility.

INTRODUCTION

In modern heavy wood structures, a frame composed of large-section columns and beams generally supports the load, and large-section timber or glulam are used as structural members. However, in the case of large-dimensional member, drying stress occurs in the timber due to the difference in MC between the surface and inner layers during drying, leading to the easy occurrence of drying defects. Based on the thinning method that is used in low value-added industries in Korea such as chip production, larch small-square timber can be fabricated into a wood material similar to large-section member by creating laminated timber through multilayering. However, in order for laminated timber to be used as a structural member, it is necessary to review the strength performance compared with other members such as glulam. According to a previous study, Lee et al (2019) evaluated the bending performance of laminated timber manufactured by bonding two small-square timbers to use as a heavy timber structural member with laminated timber and various reinforcements. As a result of the experiment, the laminated timbers showed sufficient potential as structural members compared with glulams. However, the joints must be considered in addition to the structural members as main factors for the design of a building. The joint is an important factor when designing a heavy timber structure using larch laminated timber. This is because it can determine the overall strength and performance, but is considered a highly vulnerable area in

extreme situations like earthquakes (Huang and Chang 2017). When a seismic load occurs on a heavy wood structure with a drift pin larch beam-column joint with slotted-in steel plates, bending moment acts. When a load exceeding tension perpendicular to grain and longitudinal shear strengths of timber, which is a particularly vulnerable point in wood, is applied, brittle failure occurs at the joint, and there is a risk of collapse of the structure (LAM et al 2008). Therefore, many studies have been conducted to suppress brittle fractures. Various reinforcement methods are implemented to solve the problems in existing joints for wood. Among them, carbon fiber-reinforced plastic (CFRP) has been widely used as a reinforcing material for wooden building members owing to its excellent strength capacity and fire resistance. Xiong et al (2017) applied a horizontal cyclic load after wrapping the CFRP around the joint to improve the lateral resistance performance of the timber beam and post structure. As a result of the experiment, the reinforcement of CFRP around the joint showed a tendency to increase the maximum strength capacity of the joint and suppress the brittle fracture. Yang et al (2019) confirmed the superior performance of CFRP by conducting cyclic tests on joints with multiple reinforcement methods for preventing the loss of joint capacity due to structural damage during earthquakes. However, Xiong et al (2017) showed disadvantages of the reinforcement method, that wrapping CFRP lowered the yield moment and ductility ratio and had

poor aesthetics. In the experiment of Yang et al (2019), the yield strength increased, but the ductility ratio decreased in some specimens. To check the effect of CFRP insertion reinforcement on the performance of wood joints, Lee (2021) conducted the bearing strength test on larch square timber inserted and reinforced with different CFRP reinforcement ratios. Additionally, the tensile shear capacity of the single-bolt joint, which was reinforced by inserting and bonding CFRP with a slit within the member by changing reinforcement positions, was examined. The bearing strength experiment confirmed that the wood bearing strength increased with the increase in the CFRP reinforcement ratio. Additionally, through the tensile-type shear strength test, it was confirmed that the insertion of CFRP reinforcement improved the maximum shear strength and yield shear strength, and there was no significant difference in bonding strength according to the insertion reinforcement position. Previous studies focused on evaluating laminated timber as a structural component or joints with reinforcement wrapped around the external joint or with insertion reinforcements. Even with insertion reinforcement, it focused on the evaluation of the joint strength of a single bolt joint. There have been few studies on the joint behavior of structures with insertion of CFRP reinforcement. In this study, cyclic tests were carried out to confirm the moment of resistance capacity according to CFRP reinforcement ratio of beam-column

joints with slotted-in steel plates of larch laminated timber.

MATERIALS AND METHODS

Specimen production

Larch laminated timber was manufactured by multi-layering Larix Kaemferi Carr small square timber, as shown in Figure 1. The modulus of elasticity of each member used to prepare the specimen was 10 GPa, the average moisture content was $16 \pm 0.9 \%$ and the average air-dried gravity was 0.52 ± 0.03 (adding coefficient of variation data for the listed sample properties). The modulus of elasticity of each member was measured using a non-destructive method by the natural frequency of the longitudinal vibration. Phenol-resorcinol-formaldehyde (PRF) adhesive was used for adhesion by applying 400 g/m^2 of the adhesive on one side with 1.0 MPa pressure (Lee et al 2019). Pre-drilling for slit and drift pin insertion in laminated timber CFRP reinforcement and steel plate insertion was precision machined with a Computer Numerical Control (CNC) pre-cutting machine (K2i 1259, Hundegger). Eight fastener holes with a diameter of 16 mm were pre-drilled in the column-beam joint to prepare the larch laminated timber specimen for the moment of resistance test. The edge distance and end-distance of the joint and row spacing between the fasteners were designed as 3.5 D (DL diameter of the drift pin, 16 mm). The SS275 drift pin, 16 mm in diameter and 170 mm in length (based on the KS D 3503 standard), was used as a beam-column joint fastener. The slotted-in steel plate was used as the joint, and the inserted SS275 steel was $440 \text{ mm} \times 220 \text{ mm}$ and 8 mm thick, a rolled steel also based on the KS D 3503. For each steel plate, 16 holes with a diameter of 17 mm were pre-drilled for the drift pin group pattern of the column-beam joint (Figure 2a). The center of the control specimen was slit to a thickness of 10 mm and a depth of 225 mm to insert a steel plate. Subsequently, the steel plate was inserted to prepare a specimen for the moment of resistance test. For Type-A and Type-B specimens, a slit with a thickness of 13 mm and a depth of 225

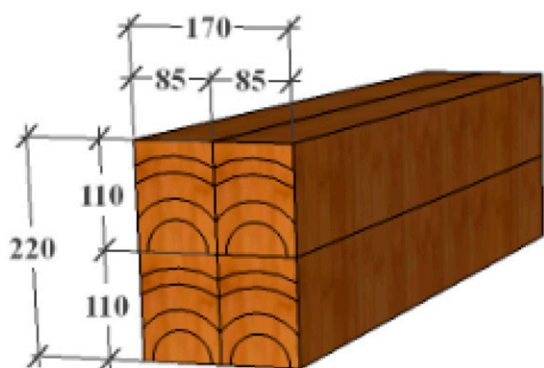


Figure 1. Production process of larch laminated timber specimens.

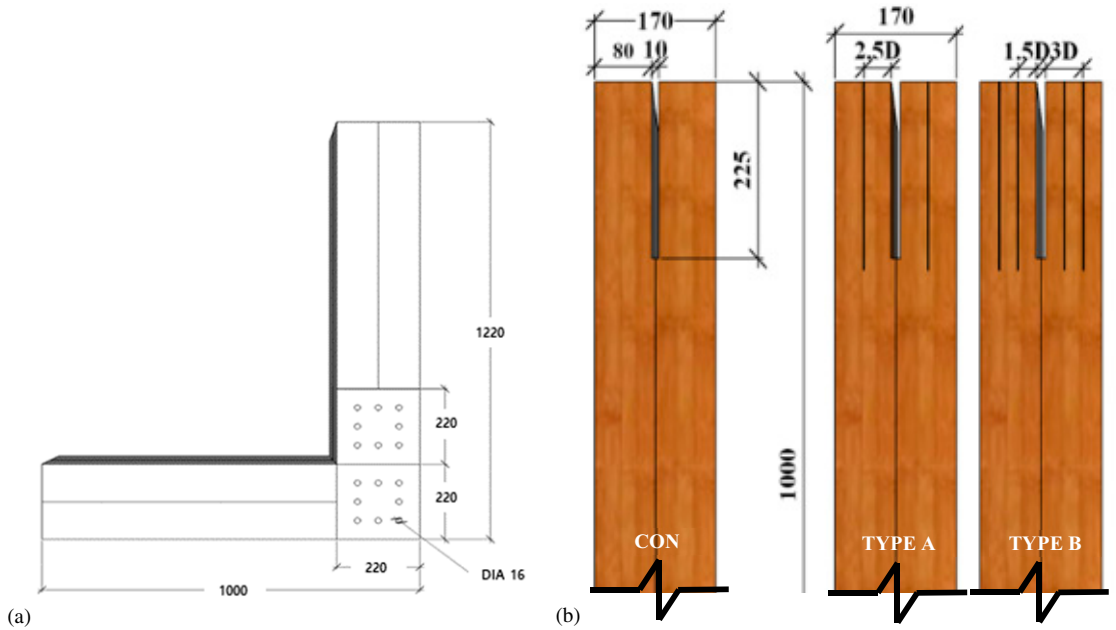


Figure 2. Schematic diagram of moment resistance specimens: (a) shape of moment resistance specimens and (b) strengthening schemes.

mm was machined in the center for reinforcement. The Type-A and Type-B moment of resistance specimens were reinforced with 1.4 mm thick carbon fiber reinforced plastic (CFRP) at the column-beam joint. The epoxy adhesive was used for joining the timber and CFRP. The Type-A specimen was prepared by inserting and joining plate-type CFRP with a thickness of 1.4 mm at 2.5D (D: diameter of drift pin, 16 mm) left and right from both sides of the steel plate slit and the slit as the starting point (volume ratio of the joint reinforced with CFRP: 3.6%). The Type-B specimen was prepared by inserting and joining the plate-type CFRP at 1.5D and 3D from both sides of the steel plate slit and the slit on the left and right (volume ratio of the joint reinforced with CFRP: 5.4%). A total of nine specimens were prepared, three for each type of moment of resistance specimens (Figure 2b).

Test Methods

Loading cell (TCL-100KNB, Tokyo Sokki Kenkyo) with 100 kN capacity was used for the cyclic test. The moment of resistance specimens

was rotated 90 degree before the test for the ease of load application of the load cell. To fix the moment of resistance specimens, the bottom part of column member was fixed onto the stopper using 12 mm bolts. Then, a cyclic load was applied from the upper right corner of the moment of resistance specimen.

A total of six 50 mm Tokyo Sokki Kenkyujo displacement transducers were used to measure the deformation caused by the moment increase of the column-beam joint of the moment of resistance specimen (Fig 3a). A data logger (TDS-302, Tokyo Sokki Kenkyujo) and a computer data acquisition system were used to identify the displacement of each displacement transducer according to changing load. Transducers were installed as shown in Fig 3a to measure the deformation according to the increase in the moment at the column-beam joint of the moment of resistance specimens. Transducer 1 was installed to measure the horizontal displacement on the opposite side of the beam, at which the load was applied. Transducers 2 and 3 were attached to the beam (D2 and D3 positioned at the center of the

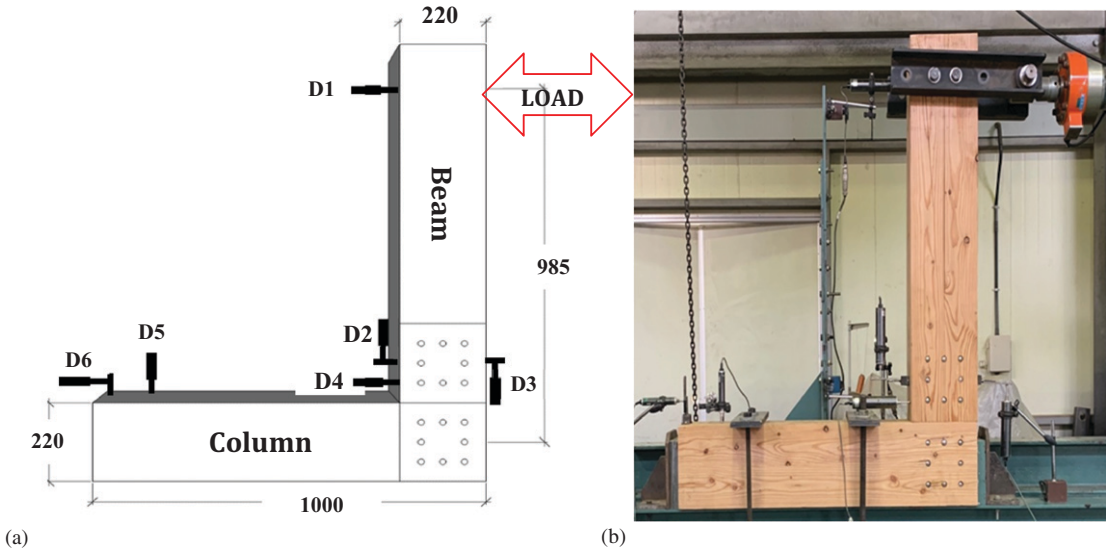


Figure 3. Test set-up for moment resistance performance test (Lee et al 2017): (a) measurement of joint rotation (schematic drawing) and (b) photograph of moment resistance specimens.

eight drift pins on the beam) and transducers 2 and 3 were installed to measure the vertical displacement. Displacement transducers 4, 5, and 6 were fixed to the lower part of the column member of the specimen with a stopper to correct occurring deformations other than joint moment deformation due to cyclic loads. The moment value was calculated with the distance from the center of rotation of the column member to the point where the horizontal force was applied (h : 985 mm) and the load applied from the load cell.

The loading protocol of the cyclic test was based on the standards of the AIJ (Architectural Institute of Japan), and the positive and negative cycles, corresponding to the rotation angles of $\pm 1/600$, $\pm 1/450$, $\pm 1/300$, $\pm 1/200$, $\pm 1/150$, $\pm 1/100$, $\pm 1/75$, and $\pm 1/50$ rad, were applied three times. The test was terminated when the load was reduced to 80% of the maximum load in the positive direction (Fig 4). Details of loading procedure for each cycle are shown in Table 1. The loading speed was set at 40 mm/min. The rotation angle (φ)

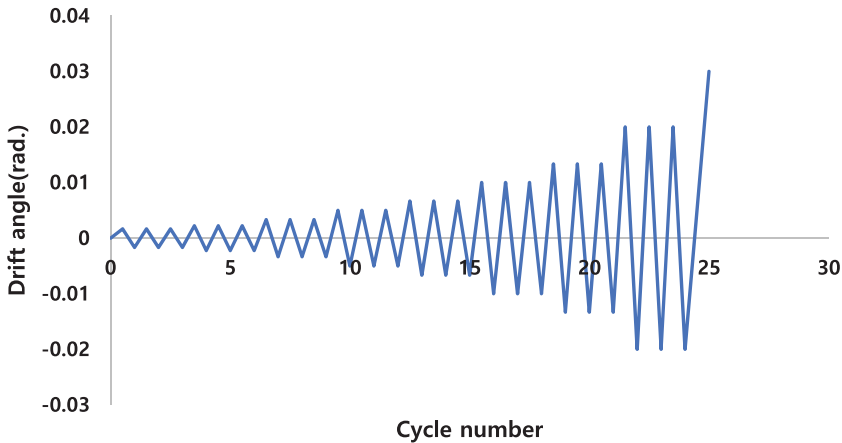


Figure 4. Loading protocol according to Architectural Institute of Japan.

Table 1. Horizontal displacement according to drift angle.

Drift angle (rad.)	Horizontal displacement (mm)	Cycle number
1/600	1.64	3
1/450	2.18	3
1/300	3.27	3
1/200	4.93	3
1/150	6.57	3
1/100	9.85	3
1/75	13.14	3
1/50	19.7	3
Failure		1

φ = Rotation angle between column and beam members; H_1 = Horizontal displacement of transducer 1; H_3 = Horizontal displacement of transducer 3; h = Distance from the center of rotation to the point where the horizontal force is applied (985 mm).

between the column and beam member was calculated by Eq 1.

$$\varphi = \tan^{-1} \left[\frac{H_1 - H_3}{h} \right] \quad (\text{Eq 1})$$

Calculation Method of Strength Properties of Joints by Elasto-Plastic Model (Bilinear Method)

The strength characteristics of the joint were calculated using the elasto-plastic model (bilinear

method) according to AIJ (Park et al 2014). The bilinear curve was originally designed for concrete and steel systems. It is assumed that the area under the test curve is the same as the area under the bilinear curve by two straight lines, and this method the behavior of the structure that separates the elastic and plastic regions (Muñoz et al 2008) (Fig 5). The envelope curves were obtained from a moment-rotation angle curve. The M_{\max} (maximum moment), θ_{\max} (maximum rotation angle), M_y (yield moment capacity), θ_y (yield rotation angle), R (rotational stiffness), M_u (ultimate moment), θ_u (ultimate moment rotation cycle), θ_v (elasto-plastic models yield point rotation angle), and μ (ductility ratio) were calculated after the envelope curves were obtained from the moment-rotation angle curve (Lee et al 2017; Beak and Jimura 2009).

RESULTS AND DISCUSSION

Evaluation of Joint Capacity

Maximum Moment and Failure mode. The moment-rotation relations were established from the load-displacement data recorded during the cyclic tests. The maximum moment was calculated from the maximum load when the forward

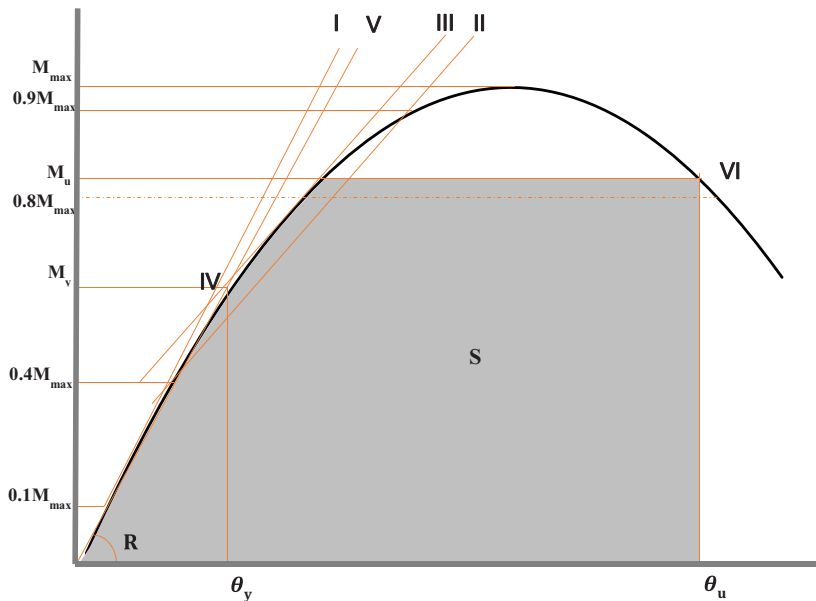


Figure 5. Estimation method for the joint capacity (Lee et al 2017).

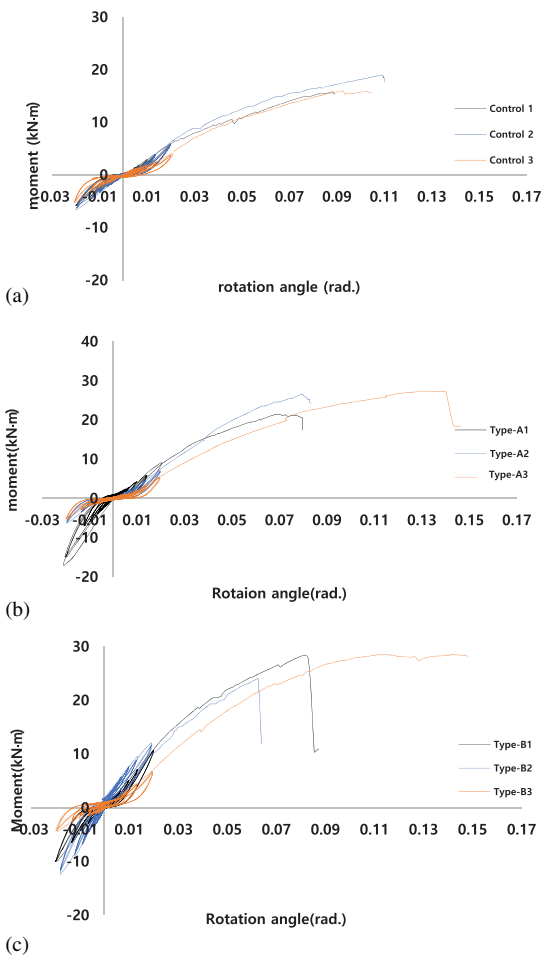


Figure 6. Moment-rotation angle curves: (a) control—non-reinforced joint, (b) Type-A—carbon fiber-reinforced plastic (CFRP) reinforcement volume ratio 3.6%, and (c) Type-B—CFRP reinforcement volume ratio 5.4%.

horizontal force was applied after repeating the positive and negative cycles three times. Figure 6 shows the moment-rotation angle curves of each specimen according to the cyclic test standard. The average maximum moment of the control specimen was 16.9 kN·m. When compared with the beam-column joint with slotted-in steel plates using glulam by Lee et al (2017) and Jung et al (2016), the applicability of the laminated timber joint was confirmed. Generally, when an external force is applied to the drift pin joint with slotted-in plates, the surface of the wood is pressed by

the drift pin, causing deformation. Deformation by such bearing significantly affects the strength and rigidity of the joint. The bearing strength refers to the yield strength per unit area when the wood is pressed by fasteners such as drift pins. For the control specimen, as the column member rotated by the horizontal force, the bearing was generated in wood, which had relatively weak bearing strength compared with the steel plate and drift pin, causing cleavage cracks in the end distance direction. As the load gradually increased, the cleavage cracks increased along the drift pin row of the column member. The rotation of the column member then generated the bearing, resulting in a secondary fracture (Fig 7a). According to Gehloff et al (2010) and Yang et al (2019), splitting failure occurred in the column-beam joint of the unreinforced moment of resistance specimen in the cyclic tests, which was also observed in the control specimen in this study. Type-A and Type-B specimens reinforced with CFRP exhibited higher maximum moments than the control specimens. The average maximum moment of the Type-A (volume ratio of the joint reinforced with CFRP: 3.6%) was 24.6 kN·m, which was improved by 46% compared with that of the control specimen. All Type-A specimens tended to suppress the splitting failure in the beam members owing to the reinforcing effect of the CFRP. In the Type-A1 specimen, cleavage cracks generated from the cross-section of the column member gradually increased along the drift pin row until the test was terminated, resulting in splitting failure after 0.07 rad, and the Type-A2 specimen exhibited a similar failure mode (Fig 7b). In Type-A3, cleavage cracks occurred, but the cleavage cracks did not increase, and splitting failure occurred after 0.14 rad. (Fig 7c).

The maximum moment of the Type-B (volume ratio: 5.4%) specimen was 27.3 kN·m, which was improved by 62% compared with that of the control specimen. In the Type-B1 specimen, the net tension failure occurred in the beam member (Fig 7d). When the structure rotated, the beam member may have received a tensile force, leading to a failure in the direction perpendicular to grain of

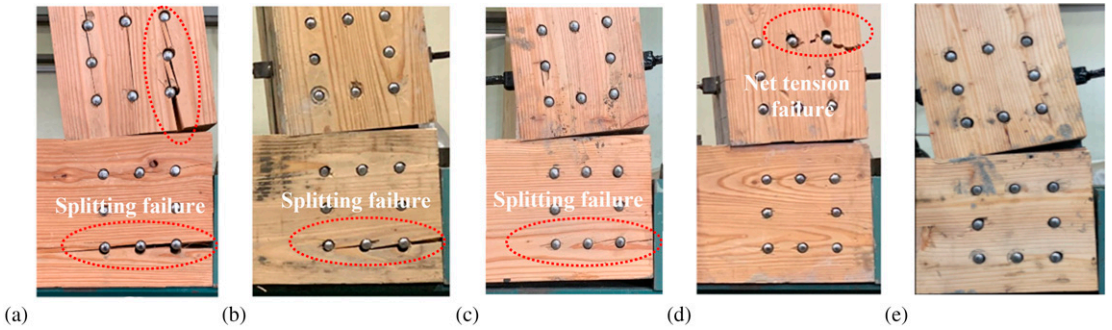


Figure 7. Failure mode of moment resistance joint specimens after test: (a) general failure mode of control specimens, (b) Type-A1, A2 specimens, (c) Type-A3 specimen, (d) Type-B1 specimen, and (e) Type-B3 specimen.

the beam member. The Type-B2 specimen exhibited splitting failure after 0.08 rad, and the failure was similar to that of the Type-A specimen. The Type-B3 specimen may have exhibited sufficient ductility because the CFRP reinforced at the joint suppressed the brittle failure of the member (Fig 7e). Thus, the CFRP suppressed the splitting failure by improving the joint capacity of the column-beam joint, showing a similar trend to the studies by Xiong et al (2017) and Yang et al (2019). Furthermore, as the reinforcement ratio of the CFRP increased, the joint capacity and ductility were improved, and the failure was suppressed in the end distance direction.

Cyclic Stiffness. When each cycle (1/600 rad. ~1/50 rad.) was repeated three times according to the cyclic test standard, high stiffness was observed in the first cycle for each cycle. However, as the cycle was repeated, the bearing was generated on the surface of the wood by the drift pin, resulting in a gap between the drift pin and wood. This gap was continuously widened as the cycle was repeated, causing a decrease in stiffness; a brittle failure may occur. When a brittle failure occurred in wood, the stiffness was significantly decreased. Figure 8 shows the cyclic stiffness for the first cycle of each cycle of the control, Type-A, and Type-B specimens. The cyclic

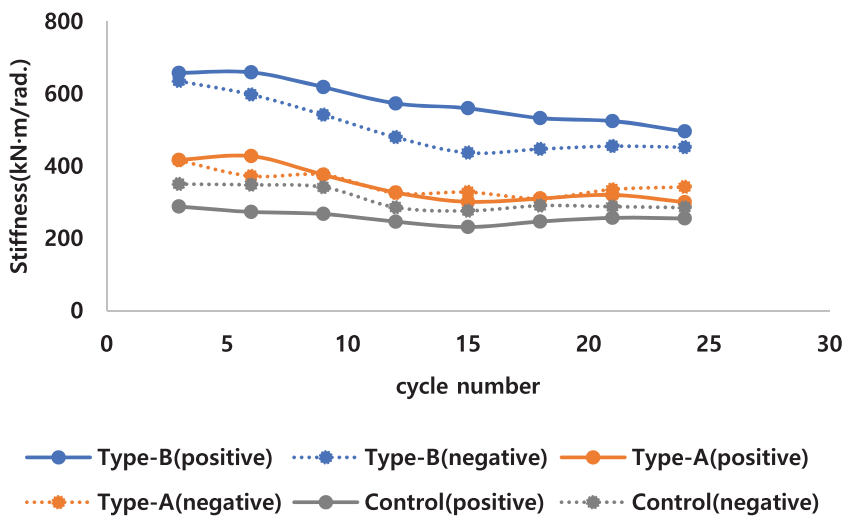


Figure 8. Stiffness variation according to the rotation angle.

stiffness, used to evaluate the stiffness degradation experienced by specimens, is calculated for each cycle as the slope of the line connecting the origin with the two points of loading corresponding to the maximum positive and negative displacements (Poletti et al 2016). Although the stiffness decreased with cyclic loading of all specimens, splitting did not appear until 1/50 rad. In this study, the stiffness tended to decrease as the test was repeated. The cyclic stiffness of the control specimen was 262.4 kN-m/rad. The Type-A and Type-B specimens showed superior cyclic stiffness than the control specimen in all sections, which were improved by 30% and 89%, respectively, compared with that of the control specimen.

Elasto-plastic analysis. When the joint is subjected to repeated loads such as earthquakes, stiffness, which is a characteristic in the elastic region, is important, but the behavior after passing the yield point is also important (Gehloff et al 2010). The ductility indicates how much deformation a structure can undergo without breakage (strength loss), and is an important evaluation index of seismic performance. Ductility is crucial in design as the ductile behavior of structures increases the ability to absorb energy if the structures exhibit ductile behaviors. The ductility is largely divided into displacement ductility and energy ductility, and in general, ductility ratio means the degree of displacement ductility. Ductility ratio was calculated through the elasto-plastic model (Table 2).

In this experiment, the ductility ratio refers to the ultimate moment angle divided by the yield

Table 2. Elasto-plastic results of the moment specimen joints.

	Control	Type-A	Type-B
M_y (kN-m)	9.3 (13.2)	13.4 (13.3)	13.7 (17.0)
θ_y (rad.)	0.037	0.034	0.028
R (kN-m/rad.)	255.6	403.9	507.3
M_{max} (kN-m)	16.9 (14.7)	24.6 (15.8)	27.3 (8.0)
θ_{max} (rad.)	0.097	0.092	0.086
M_u (kN-m)	15.86	21.68	22.57
θ_u (rad.)	0.13	0.125	0.117
θ_v (rad.)	0.061	0.055	0.047
μ	2.13	2.27	2.48

moment rotation angle of the elasto-plastic model. For the reinforcement of the column-beam joint, Lam et al (2008) reinforced the self-tapping screw to improve the joint capacity and ductility of the dowel-type column-beam joint with slotted-in steel plates. They determined that the maximum moment and yield moment were improved by 75% and 22%, respectively, compared with that of the nonreinforced joint. Compared with the reinforcement method of Yang et al (2019) and Xiong et al (2017), the insertion reinforcement effect was slightly improved. In this study, the Type-A and Type-B specimens reinforced with CFRP exhibited superior strength and stiffness than the control specimen. The yield moment of the control specimen was 9.3 kN-m, the ultimate moment was 15.86 kN-m, and the ductility ratio was 2.13. The Type-A specimen showed an improved yield moment by 43% and cyclic stiffness by 58% compared with the control specimen, and the ductility factor was approximately 7% higher.

The Type-B specimen showed the highest joint capacity, and the yield moment was not significantly different from that of the Type-A specimen. However, the cyclic stiffness and ductility rate were 98% and 17% higher than those of the control specimen, respectively. Through this, it was confirmed that the yield moment and ductility ratio were improved as the reinforcement ratio of CFRP increased.

CONCLUSION

#1. Laminated timber is a wood composite made by multiple-layering of small-square timber. Unreinforced laminated timber moment of resistance specimen showed similar moment of resistance performance and failure mode as glulam specimen, which confirmed the potential use of laminated timber structures.

#2. The improvement in the bearing strength of the wood in the moment of resistance specimen was achieved through the insertion of CFRP reinforcement. This effect restrained the generation of a change in bearing from a large stiffness difference between the wood and metal fastener, which

restrained splitting. Accordingly, high stiffness and the maximum moment capacity were gained.

#3. The reinforcement effects of CFRP were observed in the initial elastic region and the plastic region. The CFRP dispersed the stress concentration at the junction, increasing the ductility ratio. Higher ductility was observed with the increase in the CFRP reinforcement ratio.

ACKNOWLEDGMENTS

This study was conducted as a basic research project supported by the Korea Research Foundation with funding from the Korean Ministry of Education in 2016 (Grant No. R1D1A1B01011163).

REFERENCES

- Beak HS, Iimura Y (2009) Development of moment resisting joints using threaded steel shaft and drift pin. *J Archit Inst Korea Struct Constr* 25(8):61-69.
- Gehloff M, Cloßen M, Lam F (2010). Reduced edge distances in bolted timber moment connections with perpendicular to grain reinforcements. *In Proceedings, World Conference on Timber Engineering*, Vol. 201.
- Huang H, Chang WS (2017) Seismic resilience timber connection—adoption of shape memory alloy tubes as dowels. *Struct Contr Health Monit* 24(10):e1980.
- Jung HJ, Song YJ, Lee IH, Hong SI (2016) Moment resistance performance evaluation of larch glulam joints using GFRP-reinforced laminated plate and GFRP rod. *J Korean Wood Sci Technol* 44(1):40-47.
- Lam F, Schulte-Wrede M, Yao CC, Gu JJ (2008) Moment resistance of bolted timber connections with perpendicular to grain reinforcements. *In Proceedings, 10th World Conference on Timber Engineering (WCTE)*.
- Lee IH, Song YJ, Hong SI (2017) Evaluation of moment resistance of rigid frame with glued joint. *J Korean Wood Sci Technol* 45(1):28-35.
- Lee IH, Song YJ, Hong SI (2021) Tensile shear strength of steel plate-reinforced larch timber as affected by further reinforcement of the wood with carbon fiber reinforced polymer (CFRP). *BioResources* 16(3):5106.
- Lee IH, Song YJ, Song DB, Hong SI (2019) Results of delamination tests of FRP-and steel-plate-reinforced Larix composite timber. *J Korean Wood Sci Technol* 47(5):655-662.
- Muñoz W, Mohammad M, Salenikovich A, Quenneville P (2008) Determination of yield point and ductility of timber assemblies: in search for a harmonised approach. *Engineered Wood Products Association*.
- Park CY, Kim H, Eom CD, Kim GC, Lee JJ (2014) Effect of lintel on horizontal load-carrying capacity in post-beam structure. *J Wood Sci* 60(1):30-38.
- Poletti E, Vasconcelos G, Branco JM, Koukouviki AM (2016) Performance evaluation of traditional timber joints under cyclic loading and their influence on the seismic response of timber frame structures. *Constr Build Mater* 127:321-334.
- Xiong H, Liu Y, Yao Y, Li B (2017) Experimental study on the lateral resistance of reinforced glued-laminated timber post and beam structures. *J Asian Archit Build Eng* 16(2):379-385.
- Yang JQ, Smith ST, Wang Z (2019) Seismic behaviour of fibre-reinforced-polymer-and steel-strengthened timber connections. *Adv Struct Eng* 22(2):502-518.